Synthetic modification of fusogenic coiled coil peptides

Crone, N.S.A.

Azobenzene crosslinking for coiled-coil photoswitching

Abstract

Azobenzene-based intramolecular crosslinkers have been shown to allow control over peptide structure through photoisomerization of the azobenzene. This crosslinking strategy was applied to a coiled-coil system previously used for membrane fusion, with the aim of introducing control in that system. Photocontrol over peptide structure could be achieved, but after combining the peptide with its complementary binding partner only a minimal difference between the initial dark and irradiated state was observed. Reducing the length of the peptide to three heptads increased the effect of the azobenzene crosslinker on peptide structure, yielding a heterodimeric coiled-coil that could be switched from 46% helicity in the dark state to 64% helicity in the light state. For further studies, alternative (synthetic) methods of crosslinking should be investigated as yields of the azobenzene-crosslinked products were low, and more effective switching of peptide structure leads to increased control over peptide activity.

4.1 Introduction

Coiled-coil motifs can be designed to self-assemble with high affinity and selectivity.[1] These properties have given them an important role in the field of synthetic biology and self-assembled nanomaterials.[2-4] The range of applications for coiled-coil peptides can be broadened by integrating specific, external triggers for their self-assembly. Specifically, active control over coiled-coil formation in the liposomal membrane fusion system developed in our group should allow control over its activity. This system consists of a heterodimeric coiled-coil that, when attached to separate lipid membranes via a cholesterol anchor and polyethylene glycol (PEG) spacer, shows membrane fusion in a manner similar to naturally occurring SNARE-proteins.[5, 6] The coiled-coil peptides are named 'E' and 'K', based on the dominant charged amino acid in their sequence. For applications in drug delivery, improving upon the existing coiled-coil fusion systems via the incorporation of external stimuli should allow precisely controlled release of carrier molecules across lipid membranes.

Stimuli-responsive systems can change their behaviour in response to an alteration in chemical or physical conditions. Specifically the binding of metal ions,[7] change in pH,[8] redox chemistry,[9] and enzymatic alteration of amino acids,[10] have been used to generate chemoresponsive coiled-coil peptides and proteins. Chemical control over self-assembly often requires precise control over experimental conditions, which is easy to achieve in laboratory settings, but does not translate well to bioactive systems. Due to the requirement for biocompatibility in combination with selectivity and ease of use, light is a popular alternative to chemical input when designing a responsive system.[11] The integration of a photoactive molecular switch also has the advantage of being reversible, either optically or thermally, and is therefore a common method of generating photoactive systems.[12, 13]

Azobenzenes are one of the most widely used photoactive switches, changing in structure upon isomerization between the planar *trans* isomer and the twisted *cis* isomer across the diazene bond (**Scheme 4.1A**). Under dark conditions, the azobenzene is predominantly *trans*, which is the most thermodynamically favoured isomer, but the ratio of isomers can be altered via light isomerization. The ratio of isomers after light irradiation depends on the quantum yield of the *trans-cis* and *cis-trans* isomerization and their extinction coefficients at the wavelength used for

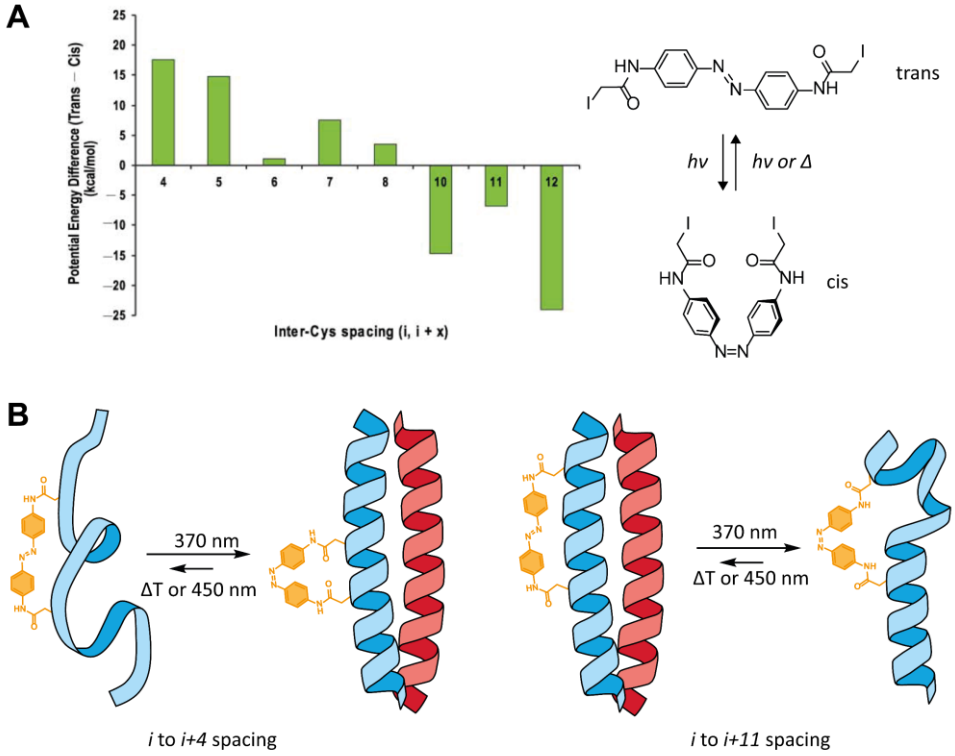

Scheme 4.1: Azobenzene based crosslinker for the photocontrol of peptide structure and the effect of crosslinker spacing on the difference in calculated peptide folding energy when switching between *cis* and *trans* isomers (A). Images adapted from Flint *et. al.*[14] Schematic representation of incorporating photoactive crosslinkers in a heterodimeric coiled-coil system (B). Depending on spacing between the attachment points of the crosslinker, either the light or the dark state can be expected to show the highest coiled-coil characteristics.

isomerization. Both of these properties can be influenced by substituents on the aromatic rings of the azobenzene. In general, the *cis* conformation is the predominant isomer when light corresponding to the π-π* absorption band is used for isomerization, while the *trans* isomer is dominant with light corresponding to the n-π* transition.[15] The isomerization changes the relative position of substituents placed on the azobenzene rings. End-to-end distance between substituents placed on the azobenzene shows a large change in distance in the *trans* conformation compared to the *cis* isomer. This change in end-to-end distance has been used successfully for the control of biomolecule activity.[16-18]

The group of Woolley extensively used azobenzene based bifunctional crosslinkers (**Scheme 4.1A**) to generate photoresponsive peptides. For example, they were able

to photocontrol the helicity of a short 16-amino acid peptide via intramolecular crosslinking of two cysteine residues.[19] By changing the inter-cysteine spacing the difference in peptide folding energy between the *trans* and *cis* isomers of the crosslinker could be altered (**Scheme 4.1A**). This allowed both states to be the predominantly folded state depending on cysteine spacing, showing the versatility of this crosslinking strategy.[14] Many alterations to this system have been made to change linker size, absorption maximum, relaxation time and solubility to tune the system for different biochemical applications, but the central mechanism of function remains the same.[20-24]

The prospect of using photoswitchable crosslinkers in coiled-coil motifs has been investigated previously, specifically in controlling the activity of basic leucine zipper proteins (bZIPs). The DNA-binding homodimeric GCN4-bZIP was modified with an azobenzene-based crosslinker and showed an increase from 40% to 90% DNA binding when isomerized with light, demonstrating changes in structure-dependent activity.[25] The transcription factor Fos was also shown to have altered activity when macrocyclized using an azobenzene crosslinker. Normally an equilibrium between the more stable Fos/Jun heterodimeric bZIP and less stable Jun/Jun homodimeric bZIP is observed; this equilibrium could be shifted using the photoactive XAFosW variant, resulting in significant differences between the irradiated and dark adapted state which were visualized using a luciferase reporter *in vitro*.[26] Recently, bifunctional azobenzene crosslinking was also used for intermolecular crosslinking of a short (14 amino acid) homodimeric coiled-coil peptide, which allowed for significant changes in peptide structure between the two isomers. [27]

In this chapter we aim to bridge the design of photocontrolled α-helices and coiled-coil proteins through the incorporation of a photoactive crosslinker in one of the helices of a synthetic heterodimeric coiled (**Scheme 4.1B**), which should in turn allow photocontrolled activation of membrane fusion. Both 'turning on', and 'turning off' coiled-coil formation by light irradiation are shown, and depend on the spacing of crosslinking sites, with the overall effectiveness of photoswitching being dependent on the length of the coiled-coil motif.

4.2 Results and Discussion

Peptide and crosslinker synthesis

Two variants of the fusogenic peptide K_4 were prepared for crosslinking via Fmoc-based SPPS(**Scheme 4.2**), incorporating two cysteine modifications which should

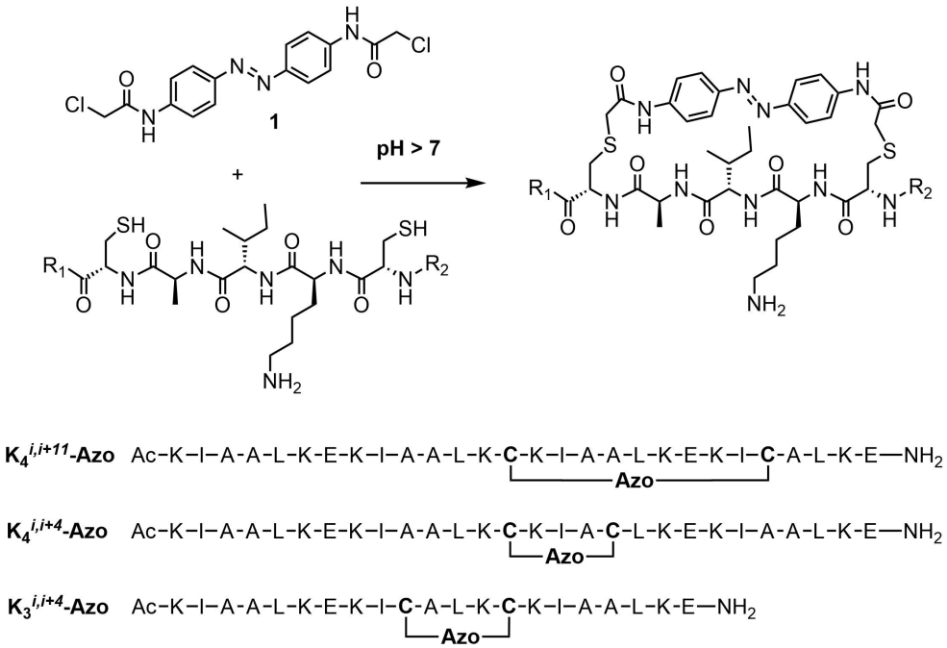

Scheme 4.2: General reaction scheme for the preparation of azobenzene-crosslinked peptides, and the sequences of the three crosslinked peptides discussed in this chapter.

allow thiol-halogen exchange with the crosslinker at neutral pH. Cysteines were positioned in the coiled-coil backbone at the centre of the peptide sequence with an *i* to *i+4* or *i* to *i+11* spacing, as this has previously been demonstrated to be optimal for helical control of this type of crosslinker.[14] The *i* to *i+4* spaced variant is designed to fold into a helical structure when the azobenzene crosslinker is in its *cis* isomer, while the *i* to *i+11* spacing is expected to yield the most helical peptide with the crosslinker in the *trans* conformation. Azobenzene based crosslinkers were prepared according to previously published literature procedures.[19] In short, 1,4-diaminobenzene was oxidized to 4,4'-diamino-azobenzene (**2**), which was reacted with chloroacetyl chloride to yield crosslinker **1** in 87% yield (reaction scheme shown in **Scheme 4.3A**). The dibromo-variant **3** could be prepared in the same manner as **1** using bromoacetyl bromide, with the diiodo variant **4** prepared through a Finkelstein substitution of **1** with sodium iodide.

An attempt was also made to synthesize the previously published azobenzene crosslinker **5** (starting from 4-nitro-3-chloroaniline, **Scheme 4.3B**) containing two pyrrolidine moieties positioned *ortho* to the diazene, which was shown to have a very fast thermal *cis* to *trans* isomerization and red-shifted absorption bands.[21]

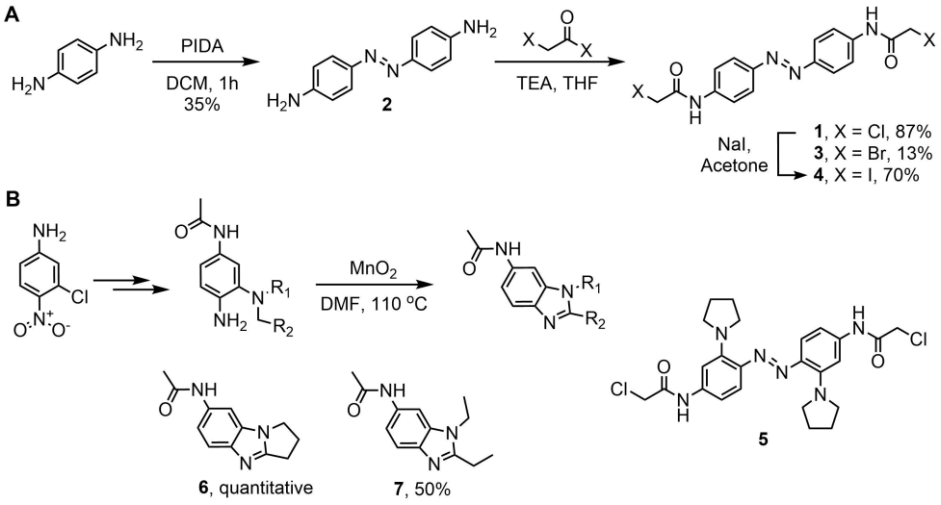

Scheme 4.3: Synthesis of azobenzene crosslinkers **1**, **3** and **4**, (A) and the attempted synthesis of crosslinker **5** showing efficient conversion of ortho-aminoalkanes to benzimidazoles (B).

Preparation of this crosslinker according to the literature procedure was deemed unsuitable, since the published yield was only 2% for oxidation of the aniline intermediate. Different reaction conditions were tested to oxidize 4-amino-3-(pyrrolidyl)acetanilide to the respective azobenzene. Conditions that formed the desired product were not found, but when manganese dioxide was used as the oxidant in DMF, an alternative reaction was observed that yielded the cyclized benzimidazole product **6** exclusively. The same conditions oxidized 4-amino-3-(diethylamino)acetanilide to benzimidazole **7** in 50% yield, showing that this reaction occurs generally for this class of compounds and these conditions might be of interest for further study into their potential synthetic application. Because no novel oxidative methods were encountered that yielded the azobenzene in good yields, the synthesis of crosslinker **5** was not pursued further.

Crosslinking of cysteine substituted peptides $K_4^{i,i+11}$-Azo and $K_4^{i,i+4}$-Azo was attempted with crosslinker **1** following literature protocols relying on thiol-halogen exchange under basic conditions (pH 7.6-8.2, **Scheme 4.2**). These conditions make use of a low peptide concentration to favour the intramolecularly crosslinked product over intermolecular crosslinking. The followed protocols generally require peptides in an unstructured state, relying on high concentrations of chemical denaturants and organic solvents to keep the hydrophobic crosslinker dissolved during the synthesis.[28] The *i* to *i+4* crosslinked variant additionally requires the azobenzene crosslinker to be in the *cis* conformation for successful incorporation,

adding illumination steps in the synthetic protocol since the *trans* isomer is thermodynamically the most stable. These protocols proved to be low-yielding and the reaction mixtures were difficult to purify, resulting in low (<2%) yield of both peptides after optimization of reaction time and illumination steps.

Photoswitching and structural analysis of photoactive K_4 derivatives

The crosslinked peptides were assumed to be in thermal equilibrium after purification and work-up, which was supported by their UV-Vis spectra showing mostly the *trans* isomer (**Figure 4.1A**). Isomerization of the azobenzene crosslinker could be achieved by irradiation with 375 nm or 385 nm light, as shown by the disappearance of the strong absorption maximum at 367 nm. These spectra are comparable to those of Flint *et al.*, which demonstrated mostly the *trans* isomer if the sample was dark adapted, transitioning to 80% of the *cis* isomer upon illumination.[14] Thermal relaxation of the *cis* isomer back to the *trans* conformation could also be studied in this manner and the thermal half-life of the *cis* state was determined to be 14 minutes for $K_4^{i,i+11}$-Azo (**Figure S4.2**), which is close to previously published half-life for this crosslinker, and 9.1h for $K_4^{i,i+4}$-Azo (**Figure 4.1B** and **4.1C**). This 40x difference in relaxation half-life is stark, in previous work only a 3x increase half-life was observed when comparing *i* to *i+4* with *i* to *i+11* spacing. The observed difference in half-life can likely be attributed to the different functions of the *cis* state in the folded helix, resulting in a geometric constraint.

The folding of peptide K_4 in an α-helical conformation is energetically favoured, with the photoswitchable crosslinker providing an energetic constraint which prevents the peptide from folding completely in the 'inactive' state (*trans* for $K_4^{i,i+4}$-Azo, *cis* for $K_4^{i,i+11}$-Azo). In turn, the peptide is applying a force on the crosslinker when the peptide is unfolded. The transition states of *trans*-azobenzene photoisomerization has experimentally been shown to decay in less than a picosecond,[29] multiple orders of magnitude faster than the potential folding speed of α-helical peptides and proteins.[30] Consequently, during the transition state the peptide can be viewed as constant and applying a structural constraint to the azobenzene crosslinker. Thermal isomerization of the azobenzene occurs via Rotation or Inversion,[15] which decreases the likelihood of the transition state resulting in the *trans* isomer. For $K_4^{i,i+4}$-Azo this results in a significantly increased half-life of the *cis* state, where for peptide $K_4^{i,i+11}$-Azo this would most likely affect the quantum yield of the *trans* to *cis* photoisomerization.

To determine the effect of crosslinking and isomeric state on peptide structure, circular dichroism (CD) spectra were recorded of azobenzene crosslinked $K_4^{i,i+11}$-Azo

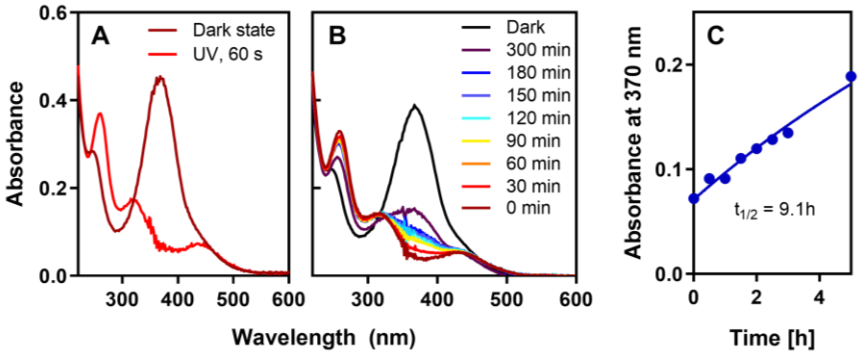

Figure 4.1: UV-Vis spectra showing the *cis* to *trans* isomerization under UV light (A), thermal back-relaxation of peptide $K_4^{i,i+4}$-Azo (B) and the fitting of this thermal relaxation (C). Peptide concentration is 50 µM in PBS, illumination performed with 375 nm light.

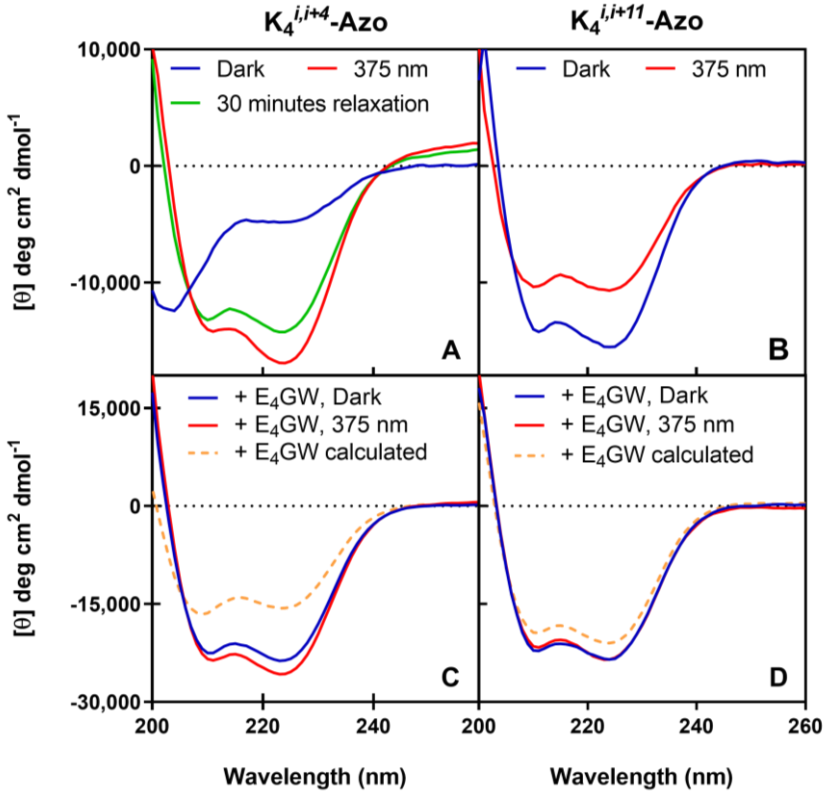

Figure 4.2: CD spectra of K_4 peptide variants crosslinked with azobenzenes. CD measurements are shown for peptide $K_4^{i,i+4}$-Azo (A) and peptide $K_4^{i,i+11}$-Azo (B) and their respective complexes with peptide E_4GW (C and D). Spectra are measured at 25 µM peptide concentration in PBS at pH 7.4, with samples either kept in the dark before measurements, or illuminated for 3 minutes with 375 nm light. Calculated coiled-coil spectra are for the less folded azobenzene isomer (*Trans* isomer for $K_4^{i,i+4}$-Azo, C; *Cis* isomer for $K_4^{i,i+11}$-Azo , D).

and $K_4^{i,i+4}$-Azo both individually and as a coiled-coil in combination with peptide E_4GW; results of these experiments can be seen in **Figure 4.2** and **Table 4.1**.$K_4^{i,i+4}$-Azo showed a random-coil structure in the initial dark state (**Figure 4.2A**), which changed to a coiled-coil like structure upon irradiation with 375 nm light. In combination with peptide E_4GW, a folded coiled-coil structure was observed for both isomers, varying from 68% average α-helicity in the initial dark state to 71% average α-helicity after light irradiation. As expected, the response of peptide $K_4^{i,i+11}$-Azo to photoisomerization was inversed, showing a coiled-coil structure which decreased from 45% to 33% average α-helicity when the azobenzene was switched to the *cis* isomer (**Figure 4.2B**, **Table 4.1**). Like the *i* to *i+4* variant, differences between the initial dark and irradiated state were minimal for the coiled coil of $K_4^{i,i+11}$-Azo with E_4GW. A clear difference can be observed between the measured coiled-coil spectra for both peptides, and the expected curves calculated by combining their independent CD absorption spectra (dashed yellow lines, **Figure 4.2C** & **4.2D**) in the dark. This increase in helicity shows coiled-coil formation, which has not been hampered by incorporation of the crosslinker in both isomeric states.

The CD experiments clearly demonstrate the premise on which the peptides were designed is indeed correct: intramolecular cysteine crosslinking using azobenzene allows for control of peptide helicity. Positioning of cysteines *i* to *i+4* shows very effective switching between an unfolded and folded helix (33% increase in average α-helicity) upon light irradiation, where cysteine positioning *i* to *i+11* allows for unfolding of the peptide when illuminated with light, although the difference is reduced with a 12% decrease in average α-helicity. These results do not translate as well to the coiled-coils, where differences between the two isomers are small for both peptides. From these CD spectra we can conclude that the geometric constraint applied by the crosslinker in the 'unfolded' state applies an energy penalty for α-helical folding. This energy penalty is larger than the folding energy of peptide K or formation of the K/K homodimer, but not larger than the energy associated with formation of the E/K heterodimeric coiled-coil. The difference in energy for the formation of the homodimer is multiple orders of magnitude lower (**Chapter 3** of this thesis) so this result is not surprising, but the observed small difference between the two isomers as a coiled-coil makes these peptides unsuitable for photocontrol of membrane fusion. To increase the difference between the two isomers, either the applied constraint needs to be amplified, or the energy of coiled-coil formation needs to be decreased to increase the effect of a single crosslinker on coiled-coil formation. Because three heptad variants of the E/K coiled-coil have already been well studied and have a lower binding energy due

to the reduction in peptide length,[31, 32] we decided to pursue azobenzene crosslinked variants of that system to achieve successful coiled-coil switching.

Synthesis and study of photoswitchable peptide $K_3^{i,i+4}$-Azo

The preparation of four heptad repeat, azobenzene crosslinked peptides was inefficient, therefore other methods were explored in the preparation of a three-heptad variant. A variant of peptide K_3 containing cysteines spaced *i* to *i+4* in the second heptad was chosen (**Scheme 4.2**) in order to optimize coupling efficiency. Different buffering conditions, solvent additives, choice and equivalents of crosslinker, illumination and reaction time were tested to increase the yield of crosslinked product with negligible improvements (**Table S4.1**). Because crosslinker **1** seemed to precipitate from solution quickly after addition started, we hypothesized the solubility of the azobenzene crosslinkers was the major bottleneck in this reaction. To overcome this, two different approaches were pursued: liquid phase coupling of the crosslinker with unprotected peptides in organic solvents, and on-resin coupling of the crosslinker to the peptide after cysteine protecting groups were selectively removed. Liquid-phase coupling was attempted with crosslinkers **1**, **3** and **4** in DMF or DMSO using DIPEA as base and showed either no reaction, or a complex mixture of products with high molecular weights, indicative of unselective crosslinking of the peptides. Coupling of the azobenzene on resin seemed to proceed well, and the desired product was a major component of the crude peptide product obtained after TFA cleavage of the peptide from the solid support; however, yields after cleavage were very low and during HPLC purification a large amount of crude material seemed to elute without giving distinguishable peaks. This leads to the conclusion that the desired products are not stable under the acidic cleavage conditions. Therefore, these two methods are not suitable for the large-scale preparation of these crosslinked peptides. Nevertheless, enough of the desired $K_3^{i,i+4}$-Azo product was isolated to analyse its viability as a photoswitching system.

The CD spectra of peptide $K_3^{i,i+4}$-Azo shows a mostly unfolded structure initially (**Figure 4.3A** and **Table 4.1,** 22% average α-helicity), which is reduced by a further 4% when isomerized to the *cis* state with 375 nm light. When this peptide is combined with its binding partner E_3GW, a clear increase in signal is observed showing absorbance bands characteristic for helical structures. A significant difference is observed between the dark adapted and irradiated state, showing an increase in average α-helicity from 46% to 64%, with the ratio of $\theta_{208nm}/\theta_{222nm}$ showing distinctive coiled-coil characteristics in the *cis* state. Photoisomerization

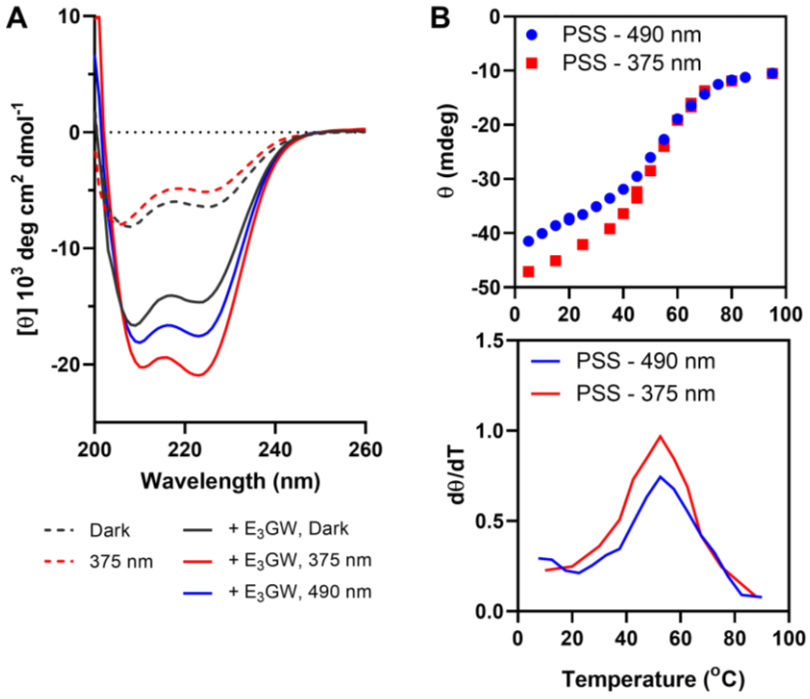

Figure 4.3: CD spectra showing the differences in folding for peptide $K_3^{i,i+4}$-Azo independently and as a coiled-coil with peptide E_3GW at different photostationary states. (A) Melt curves of the coiled-coil after isomerization with either 375 nm or 490 nm light (B, top graph) and the first order derivative of these melt spectra (B, bottom graph). Spectra were recorded in PBS buffer at pH 7.4, with 50 µM total peptide concentration.

back to the *trans* isomer can be achieved using 490 nm light, with the UV absorption of the azobenzene switching back 89% of the dark state (see **Figure S4.1**). The CD spectrum recorded after illumination with 490 nm light shows a higher degree of folding than would be expected from the combined spectra observed for the dark state and PSS at 375 nm. This suggests the coiled-coil formation of these crosslinked peptides could be partially cooperative, or contain non-dimeric intermediates that overall show a higher degree of folding then observed for the initial dark state.

Thermal denaturation experiments comparing two photostationary states (**Figure 4.3B**, **Figure S4.3**) shows the melting behaviour is only distinct in the lower temperature range. The melting point is the same for both photostationary states, indicating comparable entropic contributions to the binding affinity. Peptide $K_3^{i,i+4}$-Azo shows significantly better coiled-coil photoswitching then the four-heptad equivalent, with 18% difference in α-helicity compared to 3% difference between the dark and light states. This difference between states is counteracted

Table 4.1. Molar ellipticity and helicity for the crosslinked derivatives of peptide K, as observed by CD.

Peptides	$(\theta)_{222nm}$ (deg cm^2 dmol·res^{-1})	% α-helix [a]	$(\theta)_{222nm}/(\theta)_{208nm}$
$K_4^{i,i+4}$-azo, dark	-4,790	17%	0.50
$K_4^{i,i+4}$-azo, 375nm	-16,927	50%	1.31
$K_4^{i,i+4}$-azo + E_4GW, dark	-23,485	68%	1.15
$K_4^{i,i+4}$-azo + E_4GW, 375nm	-24,550	71%	1.16
$K_4^{i,i+11}$-azo, dark	-15,211	45%	1.31
$K_4^{i,i+11}$-azo, 375nm	-10,572	33%	1.07
$K_4^{i,i+11}$-azo+ E_4GW, dark	-23,116	67%	1.19
$K_4^{i,i+11}$-azo+ E_4GW, 375nm	-23,264	68%	1.21
$K_3^{i,i+4}$-azo dark	-6,293	22%	0.77
$K_3^{i,i+4}$-azo 375nm	-4,981	18%	0.67
$K_3^{i,i+4}$-azo + E_3GW, dark	-14,599	46%	0.88
$K_3^{i,i+4}$-azo + E_3GW, 375nm	-21,001	64%	1.11
$K_3^{i,i+4}$-azo + E_3GW, 490nm	-17,505	54%	1.00

[a] Percentage helicity was calculated from the molar ellipticity at 222 nm using Equation 2 (see materials and methods).

by a decrease in overall helicity of the irradiated state of peptide $K_3^{i,i+4}$-Azo, which indicates total fusion rates will likely be lower for this variant. If the peptide is still effective in this application remains to be determined. For this investigation, a different peptide crosslinking protocol than the one set out in this chapter will be required, due to the low yields of the crosslinking reaction.

4.3 Conclusions and outlook

Azobenzene crosslinker **1** was successfully prepared according to literature procedures, and attempts to prepare azobenzene crosslinker **5** revealed an interesting side-reaction that produced benzimidazoles from *ortho*-(alkylamino)-anilines. Since benzimidazoles are commonly used motifs, a novel mild condition for their generation would be of synthetic interest and should therefore be pursued further.

Variants of peptide K_3 or K_4 crosslinked with **1** could be photoisomerized effectively and showed clear differences in structure either individually, for the four heptad sequences, or as a coiled-coil for the three-heptad variant. This demonstrates how binding strength affects structural control of photoswitchable crosslinkers, and shows previous optimization of cysteine spacing in single helices extends to coiled-

coil motifs.[14] The structural differences show the feasibility of using photocontrol over coiled-coil structure in applications that would benefit from mediation of coiled-coil binding strength.

The methods used in this chapter for the preparation of photoswitchable peptides using crosslinkers 1, 3 or 4 are not optimal due to low yields. Other methods should therefore be explored to continue with this line of research. Specifically, the azobenzene-derivative of phenylalanine published by Hoppmann *et al.*[33] (**Scheme 4.4A**) would appear to be a suitable alternative. This amino acid contains a thiol-reactive pentafluorophenyl ring which is reactive to nucleophilic aromatic substitution (SnAr) by thiols under mild conditions. Incorporation of this amino acids omits the first reaction step of bi-reactive crosslinkers such as **1**, which negates any problems related to solubility. The crosslinker of Hoppmann *et al.* showed good reactivity towards SnAr by cysteine thiols and was successfully incorporated in the Calmodulin (CaM) protein by genetic code expansion (**Scheme 4.4B**). Photoisomerization of the azobenzene allowed control over the interactions of the crosslinked CaM protein with neuronal nitric oxide synthase, a CaM-binding protein, showing this crosslinking strategy as effective for this model system.

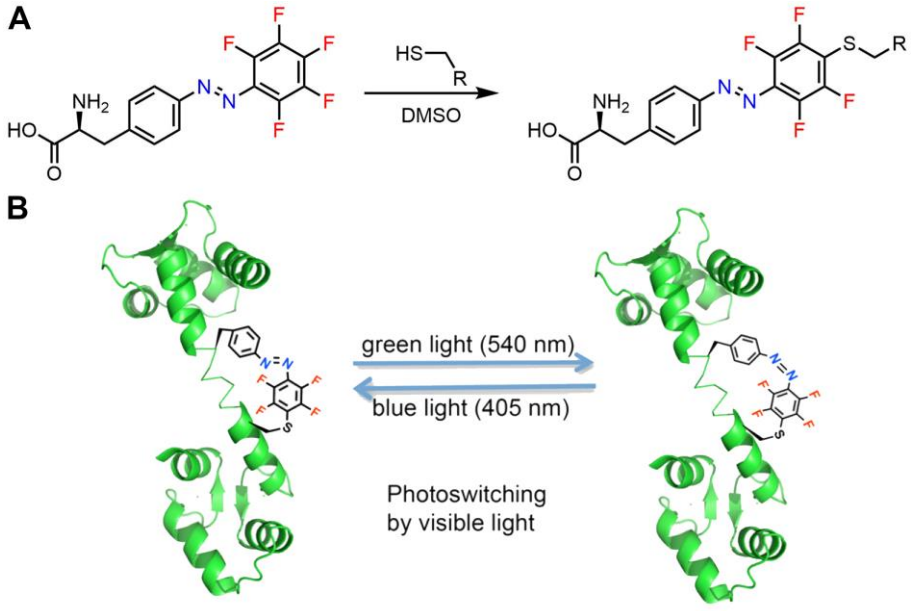

Scheme 4.4: Reaction of 4-(pentafluorophenyl)azo-l-phenylalanine with free thiols via nucleophilic aromatic substitution (A), and the application of this amino acid in the photomodulation of Calmodulin (B). Images adapted from Hoppmann *et. al.,* 2015.[33]

If the alternative crosslinker suggested above shows the same capability of controlling coiled-coil structure as the azobenzene crosslinker tested in this chapter, it would be interesting to try generating lipidated variants of these photoswitching peptides to test the hypothesis that this strategy can be used for photocontrolled membrane fusion.

4.4 Materials and Methods

Fmoc-protected amino acids were purchased from Novabiochem (Amsterdam, The Netherlands). Acetic anhydride (Ac_2O), acetonitrile (MeCN), dimethylformamide (DMF), piperidine, pyridine, trifluoroacetic acid (TFA) and tetrahydrofuran (THF) were purchased from Biosolve (Valkenswaard, The Netherlands). Oxyma was purchased from Carl Roth (Karlsruhe, Germany). p-phenylendiamine , triethyl-amine, (diacetoxyiodo)-benzene, chloroacetyl chloride, bromoacetyl bromide, sodium iodide, N,N'-diisopropylcarbodiimide (DIC) and 1,2-Bis(2-mercaptoethoxy)-ethane (EODT) were purchased from Sigma Aldrich (Zwijndrecht, The Netherlands). Manganese dioxide (MnO_2) was purchased from Alfa Aesar (Kandel, Germany). Chloroform, dichloromethane (DCM), ethyl acetate (EtOAc), ethanol and diethyl ether (Et_2O) were supplied by Honeywell (Meppel, The Netherlands). All reagents were used as purchased. Ultrapure water was purified using a Milli-Q™ purification system from Millipore (Amsterdam, The Netherlands). NMR spectra were recorded on a Bruker AV-400 (400 MHz) or AV-300 (300 MHz) spectrometer. Chemical shift values are reported in ppm relative to the solvent signal (for ^{1}H: DMSO δ= 2.50, MeOH δ= 3.31; for ^{13}C : DMSO δ= 39,52, MeOH δ= 49), with multiplicity (s = singlet, d = doublet, dd = doublet of doublets, t = triplet, q = quartet, m = multiplet), coupling constants *J* (Hz) and relative integration.

Peptide Synthesis and purification Peptides were prepared via Fmoc-based SPPS on a 0.1 mmol scale using a Liberty Blue (CEM corporation) microwave-assisted synthesizer. Synthesis was performed using Tentagel S Ram resin (Rapp Polymere, Tuebingen, Germany) with a loading of 0.23 mmol/g. Fmoc deprotection was performed with 20% piperidine at 87˚C for 1 minute and amino acid coupling was achieved using 5 equivalents of Fmoc-protected amino acid, DIC and Oxyma pure at 87˚C for 4 minutes. After synthesis, peptides were acetylated using Ac_2O and pyridine in DMF, and cleaved form the solid support using TFA containing 2.5% each of water, TIS and EODT as scavengers. After 90 minutes peptides were precipitated in cold Et_2O, dried under a stream of air, and lyophilized. Peptides were purified using reversed-phase HPLC on a Shimadzu system consisting of two KC-20AR pumps

and an SPD-20A or SPD-M20A detector, equipped with a Kinetix Evo C18 column. Purification was achieved using non-linear gradients from 10-90% MeCN in H_2O with 0.1% TFA as buffering agent. Purity was confirmed via LC-MS on a Thermo Scientific TSQ quantum access MAX mass detector connected to an Ultimate 3000 LC system fitted with a 50x4.6 mm Phenomenex Gemini 3 µm C18 column. Pure fractions were pooled and lyophilized to yield the peptides as a dry powder.

Azobenzene coupling The coupling of crosslinker **1** to double-cysteine peptides was performed by first dissolving the peptides in 50% 10 mM pH 8.0 phosphate buffer/MeCN, at 500 µM peptide concentration, followed by addition of 1.5 eq. TCEP (10 mg/mL stock solution). After 30 minutes, crosslinker **1** was dissolved in DMSO (5 mg/mL), illuminated with 375nm light to isomerize the azobenzene, and 1.5 eq. of the crosslinker is added dropwise to the peptide solution. This is repeated 3 times, for a total of 4.5 eq. of crosslinker. After 2 hours the reaction is illuminated with 375 nm light for 10 minutes to isomerize the azobenzene, then left to react overnight. The reaction was stopped by treating it with 5% TFA, centrifuged to remove any solids and purified over HPLC.

UV-Vis spectroscopy Absorption spectra were measured on an Agilent Cary-300 spectrophotometer with a scanning speed of 600 nm/min and a switchover between the visible and ultraviolet lamp at 350 nm. Samples were measured in quartz cuvettes with a path length of 10 mm and baseline corrected using a blank sample of the same solvent used for sample preparation. During measurement, samples were kept at room temperature (20˚C) using an Agilent Cary temperature controller.

CD Spectroscopy Circular dichroism spectra were recorded on a JASCO J-815 spectrometer fitted with a Peltier temperature controller. Spectra were recorded in a 2 mm quartz cuvette at 20˚C, with peptides dissolved in PBS at pH 7.4 unless otherwise specified. A wavelength range form 190-260 nm was used, with 1 nm intervals and a scanning speed of 100 nm/min, with the final spectrum consisting of the average of 5 sequentially recorded spectra, and spectra were baseline corrected using individually recorded spectra of the same buffer used for sample preparation. The mean residue molar ellipticity (θ, deg cm^2 $dmol.res^{-1}$) was calculated according to equation 1:

$$[\theta] = (100 * [\theta]_{obs})/(c * n * l) \qquad (1)$$

With [θ]obs representing the observed ellipticity in mdeg, c the peptide concentration in mM, n the number of peptide bonds and l the path length of the cuvette in cm. The fraction of α-helical peptide could be calculated from the MRE using equation 2:

$$F_{helix} = ([\theta]_{222} - [\theta]_0)/([\theta]_{max} - [\theta]_0) \qquad (2)$$

With the maximum theoretical mean residue ellipticity, $[\theta]_{max}$, defined as $[\theta]_{max} = [\theta]_\infty (n - x)/n$ for a helix with *n* residues and *x* a number of amino acids assumed not to participate in helix formation (in this case 3). $[\theta]_\infty$ is defined as the theoretical helicity of an infinite α-helix and is temperature dependent, defined via $[\theta]_\infty = (-44000 + 250T)$, with *T* being the temperature in °C. The minimal expected absorbance at 222 nm for a random coil is defined in $[\theta]_0$, which is also temperature dependent via the relationship $[\theta]_0 = 2220 - 53T$.

Sample illumination High-power single chip LEDs were purchased from Roithner Laser (Vienna, Austria) from the H2A1 series. LEDs were mounted on an aluminum back plate for heat dissipation, and powered at 350 mA current using a driver built in-house. For illumination the LED was placed parallel to the side of the cuvette at a distance of 5 mm, centered to the width and height of the sample.

Organic synthesis

Synthesis of **2** was adapted from the procedure of Ma *et al.*,[34] and the synthesis of cross-linkers was based on previous work.[19]

4,4'-Diaminoazobenzene (2): To a solution of 3.24 g p-phenylendiamine (30 mmol) in 175 mL DCM was added (diacetoxyiodo)-benzene (9.77 g, 30.3 mmol) under vigorous stirring and an immediate colour change to amber then black was observed. After 1h, the mixture was purified by silica column chromatography. The product was eluted using a gradient of 5 to 30% EtOAc in DCM and solvent was removed under reduced pressure to yield 1.11 g (5.23 mmol, 35%) of the product as a red, micro-crystalline powder. **^{1}H NMR** (400 MHz, DMSO-d_6) δ 7.53 (d, *J* = 8.7 Hz, 4H), 6.63 (d, *J* = 8.7 Hz, 4H), 5.75 (s, 4H). **^{13}C NMR** (101 MHz, DMSO- d6) δ 151.00, 143.14, 123.81, 113.4

4,4'-Di(chloroacetamido)azobenzene (1): Diaminoazobenzene (200 mg, 0.94 mmol) was dissolved in 10 mL dry THF and cooled to 5 ˚C. Triethylamine (400 µL, 2.85 mmol) and chloroacetyl chloride (250 µL, 3.07 mmol) were added and the reaction was stirred for 20 minutes. The reaction was diluted with 30 mL cold water,

the precipitate that formed was filtered off and washed 3 times with 20 mL water. The precipitate was removed from the filter with 150 mL hot acetone, and solvent was removed under reduced pressure to yield 298 mg (0.82 mmol, 87%) of the product as a brown coloured powder. **^{1}H NMR** (400 MHz, DMSO-d_6) δ 10.65 (s, 1H), 7.88 (d, *J* = 8.5 Hz, 1H), 7.81 (d, *J* = 8.6 Hz, 1H), 4.31 (s, 1H). **^{13}C NMR** (101 MHz, DMSO-d_6) δ 165.07, 148.00, 141.20, 123.55, 119.63.

4,4'-Di(bromoacetamido)azobenzene (3): Diaminoazobenzene (228 mg, 1.08 mmol) was dissolved in 15 mL dry THF and cooled to 5˚C. Triethylamine (450 µL, 3,23 mmol) and bromoacetyl bromide (400 µL, 4.06 mmol) in 5 mL THF were added, resulting in an immediate precipitate. The reaction was stirred for 10 minutes, followed by quenching with 20 mL 1:1 EtOH/H_2O. The precipitate was filtered off and washed 3 times with 20mL 1:1 EtOH/H2O. The precipitate was removed from the filter with 100 mL hot acetone, and solvent was removed under reduced pressure to yield 63 mg (0.14 mmol, 13%) of the product as a brown solid. **^{1}H NMR** (400 MHz, DMSO-d_6) δ 10.73 (s, 2H), 7.88 (d, *J* = 8.5 Hz, 4H), 7.80 (d, J = 8.6 Hz, 4H), 4.09 (s, 4H). **^{13}C NMR** (101 MHz, DMSO-d_6) δ 165.26, 148.00, 141.32, 123.57, 119.54, 30.38.

4,4'-Di(iodoacetamido)azobenzene (4): Sodium iodide (272 mg; 1.81 mmol; 7 eq.) was dissolved in a 4 ml mixture of 25 % dry THF and dry acetone. This solution was added to 60 (0.16 mmol) mg of 4,'4-di(chloroacetylamino)azobenzene and stirred under argon and protected from light for 20 hours. The reaction mixture was filtered and the solvent was evaporated under reduced pressure resulting in a brown/yellow solid. The crude product was dissolved in 2 ml of THF and cold water was added until precipitation formed. The suspension was filtered and the residue dissolved in acetone. Evaporation of the solvent yielded in 68 mg of the desired product (0.124 mmol, 70%) as a brown solid. **^{1}H NMR** (400 MHz, DMSO-d_6) δ 10.72 (d, *J* = 41.7 Hz, 2H), 7.82 (d, *J* = 28.4 Hz, 8H), 3.87 (s, 4H). **^{13}C NMR** (101 MHz, DMSO-d_6) δ 167.10, 154.14, 147.86, 123.54, 119.36, 39.52, 1.41

N-(2,3-dihydro-1H-pyrrolo[1,2-a]benzimidazol-6-yl)acetamide (6): In a 10 ml pressure vial, 11 mg 4-amino-3-(pyrrolidyl)phenyl-acetamide (0.05 mmol) and 45 mg MnO_2 (0.52 mmol; 10 eq.) was combined with 2 ml dry DMF. The vial was sealed and the reaction mixture was stirred at 110 °C for 20 hours. After all of the amine had reacted according to TLC, the mixture was filtered over Celite and the filter washed with DMF. After the solvent was evaporated under reduced pressure, the crude product was purified by silica column chromatography which yielded 11 mg

of product **6** (quantitative yield). **^{1}H NMR** (400 MHz, MeOD-d_4) δ 7.92 (d, *J* = 1.9 Hz, 1H), 7.47 (d, *J* = 8.7 Hz, 1H), 7.13 (dd, J = 8.7, 2.0 Hz, 1H), 4.14 (t, *J* = 7.1 Hz, 2H), 3.03 (t, J = 7.6 Hz, 2H), 2.78 – 2.69 (m, 2H), 2.15 (s, 3H). **^{13}C NMR** (101 MHz, MeOD-d_4) δ 171.54 (s), 145.40 (s), 142.75 (s), 134.88 (s), 119.20 (s), 116.39 (s), 103.36 (s), 44.01 (s), 27.02 (s), 24.13 (s), 23.77 (s). **TOF-MS**: [M+H]+ = 216.1135; calculated [M+H]+ = 216.1059

N-(1-ethyl-2-methyl-1H-benzo[d]imidazol-6-yl)acetamide (7): In a 10 ml pressure vial, 10 mg N-(4-amino-3-(diethylamino)phenyl)acetamide, 0.05 mmol, and 40 mg MnO_2 (0.50 mmol, 10 eq.) were combined with 2 ml dry DMF. The vial was sealed and stirred for 20 hours at 110 °C. After all of the amine had reacted, according to TLC, the mixture was filtered over Celite and the filter was washed with DMF. After the solvent was evaporated under reduced pressure, the crude product was purified by silica column chromatography, which yielded 5 mg (0.025, 50%) of product **6**. **^{1}H NMR** (300 MHz, MeOD-d_4) δ 7.97 (d, *J* = 1.5 Hz, 1H), 7.46 (d, *J* = 8.6 Hz, 1H), 7.15 (dd, *J* = 8.6, 1.8 Hz, 1H), 4.23 (q, *J* = 7.3 Hz, 2H), 2.59 (s, 3H), 2.16 (s, 3H), 1.40 (t, 3H).

4.6 References

1. Lapenta, F.*, et al.* (**2018**) Coiled coil protein origami: from modular design principles towards biotechnological applications. *Chem. Soc. Rev. 47*, 3530-3542.
2. Marsden, H. R., and Kros, A. (**2010**) Self-Assembly of Coiled Coils in Synthetic Biology: Inspiration and Progress. *Angew. Chem. Int. Edit. 49*, 2988-3005.
3. Wu, Y. Y., and Collier, J. H. (**2017**) alpha-Helical coiled-coil peptide materials for biomedical applications. *WIREs Nanomed Nanobiotechnol. 9*, e1424.
4. Utterström, J.*, et al.* (**2021**) Coiled coil-based therapeutics and drug delivery systems. *Adv. Drug Del. Rev 170*, 26-43.
5. Marsden, H. R., Tomatsu, I., and Kros, A. (**2011**) Model systems for membrane fusion. *Chem. Soc. Rev. 40*, 1572-1585.
6. Robson Marsden, H.*, et al.* (**2013**) Controlled liposome fusion mediated by SNARE protein mimics. *Biomat. Sci. 1*, 1046-1054.
7. Dublin, S. N., and Conticello, V. P. (**2008**) Design of a selective metal ion switch for self-assembly of peptide-based fibrils. *J. Am. Chem. Soc. 130*, 49-51.
8. Zimenkov, Y.*, et al.* (**2006**) Rational design of a reversible pH-responsive switch for peptide self-assembly. *J. Am. Chem. Soc. 128*, 6770-6771.
9. GarciaEcheverria, C. (**1996**) Disruption of coiled coil formation by methionine oxidation. *Bioorg. Med. Chem. Lett. 6*, 229-232.
10. Szilak, L., Moitra, J., and Vinson, C. (**1997**) Design of a leucine zipper coiled coil stabilized 1.4 kcal mol(-1) by phosphorylation of a serine in the e position. *Protein Sci. 6*, 1273-1283.

11. Ankenbruck, N., *et al.* (**2018**) Optochemical Control of Biological Processes in Cells and Animals. *Angew. Chem. Int. Edit. 57*, 2768-2798.

12. Szymanski, W., *et al.* (**2013**) Reversible Photocontrol of Biological Systems by the Incorporation of Molecular Photoswitches. *Chem. Rev. 113*, 6114-6178.

13. Pianowski, Z. L. (**2019**) Recent Implementations of Molecular Photoswitches into Smart Materials and Biological Systems. *Chem. Eur. J. 25*, 5128-5144.

14. Flint, D. G., *et al.* (**2002**) Using an azobenzene cross-linker to either increase or decrease peptide helix content upon trans-to-cis photoisomerization. *Chem. Biol. 9*, 391-397.

15. Bandara, H. M. D., and Burdette, S. C. (**2012**) Photoisomerization in different classes of azobenzene. *Chem. Soc. Rev. 41*, 1809-1825.

16. Beharry, A. A., and Woolley, G. A. (**2011**) Azobenzene photoswitches for biomolecules. *Chem. Soc. Rev. 40*, 4422-4437.

17. Mart, R. J., and Allemann, R. K. (**2016**) Azobenzene photocontrol of peptides and proteins. *Chem. Commun. 52*, 12262-12277.

18. Zhu, M. Y., and Zhou, H. C. (**2018**) Azobenzene-based small molecular photoswitches for protein modulation. *Org. Biomol. Chem. 16*, 8434-8445.

19. Kumita, J. R., Smart, O. S., and Woolley, G. A. (**2000**) Photo-control of helix content in a short peptide. *P. Natl. Acad. Sci. USA 97*, 3803-3808.

20. Zhang, Z. H., *et al.* (**2003**) A water-soluble azobenzene cross-linker for photocontrol of peptide conformation. *Bioconjugate Chem. 14*, 824-829.

21. Sadovski, O., *et al.* (**2009**) Spectral Tuning of Azobenzene Photoswitches for Biological Applications. *Angew. Chem. Int. Edit. 48*, 1484-1486.

22. Chi, L., Sadovski, O., and Woolley, G. A. (**2006**) A blue-green absorbing cross-linker for rapid photoswitching of peptide helix content. *Bioconjugate Chem. 17*, 670-676.

23. Beharry, A. A., Sadovski, O., and Woolley, G. A. (**2008**) Photo-control of peptide conformation on a timescale of seconds with a conformationally constrained, blue-absorbing, photo-switchable linker. *Org. Biomol. Chem. 6*, 4323-4332.

24. Samanta, S., *et al.* (**2013**) Photoswitching Azo Compounds in Vivo with Red Light. *J. Am. Chem. Soc. 135*, 9777-9784.

25. Woolley, G. A., *et al.* (**2006**) Reversible photocontrol of DNA binding by a designed GCN4-bZIP protein. *Biochem. 45*, 6075-6084.

26. Zhang, F. Z., *et al.* (**2010**) Photocontrol of Coiled-Coil Proteins in Living Cells. *Angew. Chem. Int. Edit. 49*, 3943-3946.

27. Torner, J. M., and Arora, P. S. (**2021**) Conformational control in a photoswitchable coiled coil. *Chem. Commun. 57*, 1442-1445.

28. Yasuike, N., *et al.* (**2019**) Intramolecular cross-linking of proteins with azobenzene-based cross-linkers. *Method. Enzymol. 624*, 129-149.

29. Fujino, T., Arzhantsev, S. Y., and Tahara, T. (**2001**) Femtosecond Time-Resolved Fluorescence Study of Photoisomerization of trans-Azobenzene. *J. Phys. Chem. A 105*, 8123-8129.

30. Kubelka, J., Hofrichter, J., and Eaton, W. A. (**2004**) The protein folding 'speed limit'. *Curr. Opin. Chem. Biol. 14*, 76-88.

31. Robson Marsden, H., *et al.* (**2009**) A Reduced SNARE Model for Membrane Fusion. *Angew. Chem. Int. Edit. 48*, 2330-2333.

32. Litowski, J. R., and Hodges, R. S. (**2002**) Designing heterodimeric two-stranded alpha-helical coiled-coils - Effects of hydrophobicity and alpha-helical propensity on protein folding, stability, and specificity. *J. Biol. Chem. 277*, 37272-37279.

33. Hoppmann, C., *et al.* (**2015**) In Situ Formation of an Azo Bridge on Proteins Controllable by Visible Light. *J. Am. Chem. Soc. 137*, 11218-11221.

34. Ma, H., *et al.* (**2012**) Organocatalytic oxidative dehydrogenation of aromatic amines for the preparation of azobenzenes under mild conditions. *Tetrahedron Letters 68*, 8358-8366.

Supporting Information for Chapter 4

UV-Vis Spectra

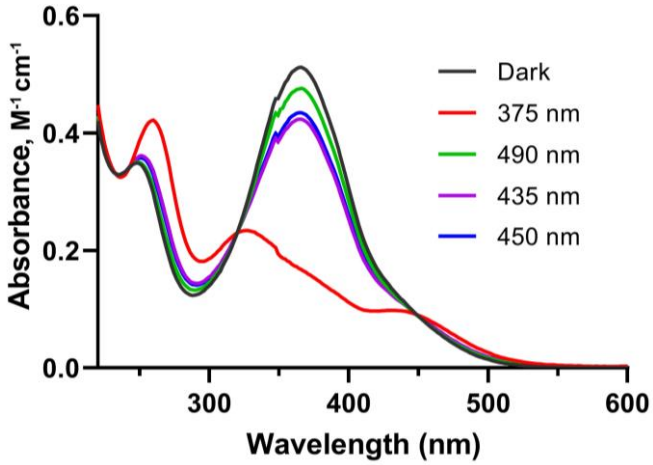

Figure S4.1: UV-Vis spectra at different photostationary states of peptide $K_3^{i,i+4}$-Azo showing successful switching between *cis*-, (375 nm) and *trans*-dominant (490 nm) photostationary states. Spectra were measured at 50 µM peptide concentration in PBS buffer, pH 7.4.

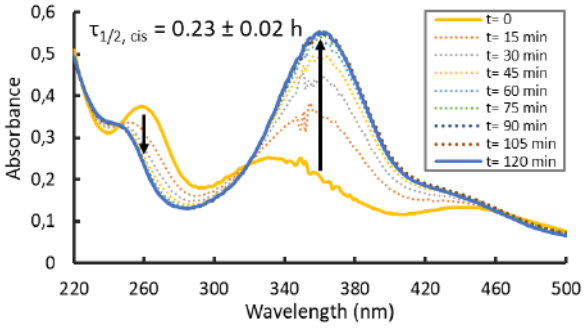

Figure S4.2: UV-Vis spectra showing the *cis* to *trans* relaxation of peptide $K_4^{i,i+11}$-Azo, 35 µM in PBS, pH 7.4. The peptide solution was irradiated with 385 nm light before relaxation was measured at a constant temperature of 25˚C. Figure adapted from the Msc. Thesis of Wessel Verbeet.

CD Spectra

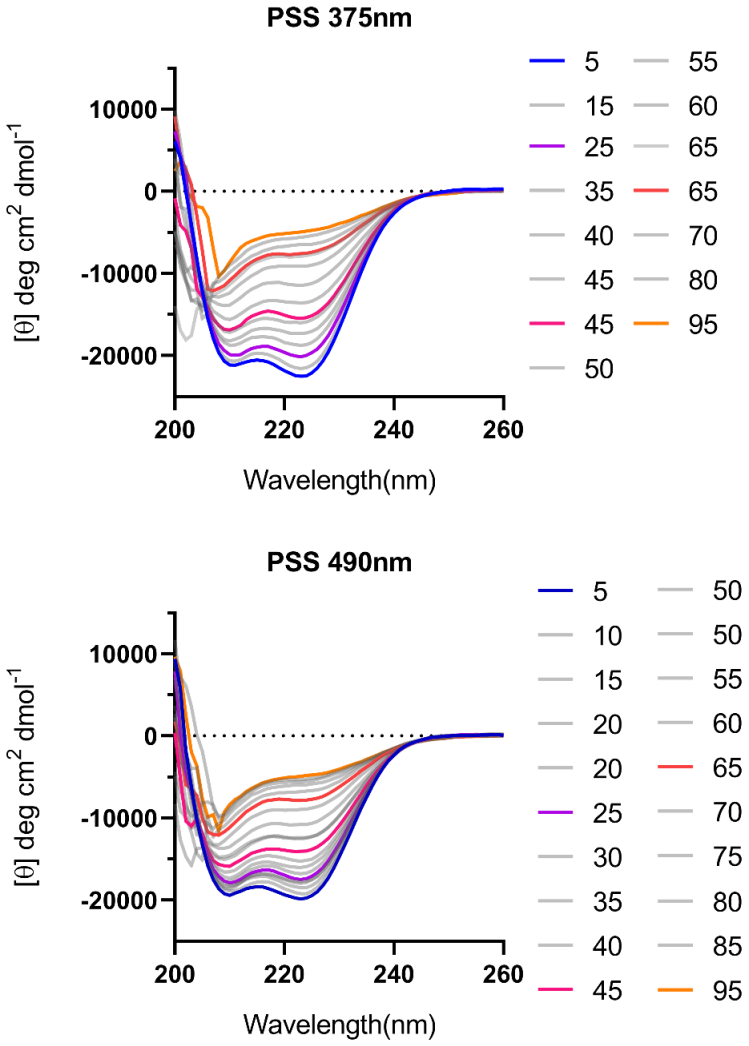

Figure S4.3: CD spectra at different temperatures (in °C) for the coiled-coil between peptide $K_3^{i,i+4}$-Azo and E_3GY at 50 µM total peptide concentration in PBS, pH 7.4. The peptide solution was irradiated with either 375 nm (top) or 490 nm (bottom) light long enough to reach the photostationary state before each measurement.

Table S4.1: Deviations from the azobenzene crosslinking protocol, and the effect on reaction outcome. Crosslinked products indicate any peptide product that has increased in mass and has an absorption band around 370 nm as observed during HPLC analysis/purification. No change indicates similar results to the crosslinking method in the materials and methods section of **Chapter 4**.

Conditions	**Effect**
Using NH_4HCO_3 or Tris buffer instead of phosphate	No change was observed
Changing peptide concentration (350 µM to 2 mM).	No change was observed
Varying the amount of crosslinker between 1.2 to 6 equivalents	Slight increase in the amount of crosslinked products, larger amounts prevent effective illumination of the sample.
Using 2M Guanidine as denaturant	Work-up was very difficult, no significant changes in yields
Using 40-60% of MeCN, DMSO, DMF, THF or ethanol as co-solvents	Slight increase in crosslinking, but increased difficulty in work-up, especially for DMF/DMSO.
Varying TCEP between 1 and 5 equivalents	No change was observed
Increasing temperature up to 50 °C	Reduced yields/more side products observed
Continuous addition of crosslinker 1 over 2 hours	No change was observed
Continuous illumination of sample for 2 hours	No change was observed
Using azobenzene crosslinker 3 or 4 to increase reactivity	Reduced yields / more side-products were observed.
Using Pyridine / 1-methylimidazole as catalysts	A decrease in peptide coupling was observed
Adding 1,2 eq. of cyclodextrin (α or β) to solubilize the azobenzene crosslinker	No change was observed

LC-MS of purified peptides

Table S4.2: Overview of the calculated masses of all peptides used in this project, and the masses found by LCMS.

Peptide name	Calculated mass (Da)	Measured mass (Da)
E_4GW	$[M + 2H^+]^{2+}$ 1661.41	1660.89
	$[M + 3H^+]^{3+}$ 1107.94	1106.94
E_3GW	$[M + 2H^+]^{2+}$ 1284.20	1284.28
	$[M + 3H^+]^{3+}$ 856.47	856.23
K_4^{i-i+11}-Azo	$[M + 2H^+]^{2+}$ 1687.48	1686.85
	$[M + 3H^+]^{3+}$ 1124.65	1124.13
K_4^{i-i+4}-Azo	$[M + 2H^+]^{2+}$ 1686.48	1688.11
	$[M + 3H^+]^{3+}$ 1124.65	1125.27
K_3^{i-i+4}-Azo	$[M + 2H^+]^{2+}$ 1311.76	1309.06